VELOCITY FILTERED DENSITY FUNCTION FOR LARGE EDDY SIMULATION OF A TURBULENT MIXING LAYER

L.Y.M. GICQUEL AND P. GIVI
Department of Mechanical and Aerospace Engineering
University at Buffalo, SUNY
Buffalo, NY 14260-4400

F.A. JABERI
Department of Mechanical Engineering
Michigan State University
East Lansing, MI 48824-1226

AND

S.B. POPE
Sibley School of Mechanical and Aerospace Engineering
Cornell University
Ithaca, NY 14853-1301

Abstract. The "velocity filtered density function" (VFDF) methodology is employed for large eddy simulation (LES) of a three-dimensional, temporally developing, turbulent mixing layer. A transport equation is derived for the VFDF in which the effects of the subgrid scale (SGS) convection appear in closed form. The unclosed terms in this equation are modeled. A system of stochastic differential equations (SDEs) which yields statistically equivalent results to the modeled VFDF transport equation is proposed. These SDEs are solved numerically by a Lagrangian Monte Carlo procedure. The VFDF results are compared with those obtained via several existing SGS closures and with data obtained by direct numerical simulation (DNS) of the mixing layer.

1. Introduction

The probability density function (PDF) approach has proven useful for large eddy simulation (LES) of turbulent reacting flows (Pope, 2000; Poinsot

and Veynante, 2001). The formal means of conducting such LES is by consideration of the "filtered density function" (FDF) which is essentially the filtered fine-grained PDF of the transport quantities (Pope, 1990). In all previous contributions, the FDF of the "scalar" quantities is considered (Pope, 1990; Gao and O'Brien, 1993; Colucci *et al.*, 1998; Réveillon and Vervisch, 1998; Garrick *et al.*, 1999; Jaberi *et al.*, 1999; James and Jaberi, 2000; Zhou and Pereira, 2000; Tong, 2001). The objective of the present work is to extend the methodology for LES of the velocity field.

2. Formulation

We consider a constant (unit) density, three-dimensional temporally developing mixing layer. The primary transport variables are the velocity vector, $u_i(\mathbf{x},t)$ $(i=1,2,3)$, and the pressure, $p(\mathbf{x},t)$, field. Large eddy simulation involves the spatial filtering operation (Guerts, 2001; Sagaut, 2001)

$$\langle f(\mathbf{x},t)\rangle_L = \int_{-\infty}^{+\infty} f(\mathbf{x}',t)G(\mathbf{x}'-\mathbf{x})d\mathbf{x}', \tag{1}$$

where $G(x)$ denotes a spatially and temporally invariant, localized and positive filter function (Vreman *et al.*, 1994) of length Δ_L, and $\langle f(\mathbf{x},t)\rangle_L$ represents the filtered value of the transport variable $f(\mathbf{x},t)$. The application of the filtering operation to the instantaneous equations describing transport of the variables in space and time (t) yields

$$\begin{aligned} \frac{\partial\langle u_i\rangle_L}{\partial x_i} &= 0, \\ \frac{\partial\langle u_j\rangle_L}{\partial t} + \frac{\partial\langle u_i\rangle_L\langle u_j\rangle_L}{\partial x_i} &= -\frac{\partial\langle p\rangle_L}{\partial x_j} + \frac{\partial\langle\sigma_{ij}\rangle_L}{\partial x_i} - \frac{\partial\tau_L(u_i,u_j)}{\partial x_i}. \end{aligned} \tag{2}$$

For a Newtonian fluid the viscous stress tensor σ_{ij} is represented by $\sigma_{ij} = \nu\left(\frac{\partial u_i}{\partial x_j}+\frac{\partial u_j}{\partial x_i}\right)$, with ν denoting the (constant) kinematic viscosity. The term $\tau_L(u_i,u_j) = \langle u_iu_j\rangle_L - \langle u_i\rangle_L\langle u_j\rangle_L$ denotes the generalized SGS stresses (Germano, 1992). The "velocity filtered density function" (VFDF), denoted by P_L, is formally defined as (Pope, 1990)

$$\begin{aligned} P_L(\boldsymbol{v};\mathbf{x},t) &= \int_{-\infty}^{+\infty} \varrho\left[\boldsymbol{v},\boldsymbol{u}(\mathbf{x}',t)\right] G(\mathbf{x}'-\mathbf{x})d\mathbf{x}', \\ \varrho\left[\boldsymbol{v},\boldsymbol{u}(\mathbf{x},t)\right] &= \prod_{i=1}^{3}\delta[v_i-u_i(\mathbf{x},t)], \end{aligned} \tag{3}$$

where δ denotes the delta function and $\boldsymbol{v}$ is the velocity state vector. The term $\varrho[\boldsymbol{v},\boldsymbol{u}(\mathbf{x},t)]$ is the "fine-grained" density (O'Brien, 1980; Pope, 1985;

Pope, 2000), and Eq. (3) defines the VFDF as the *spatially filtered* value of this density. With the condition of a positive filter kernel (Vreman *et al.*, 1994), P_L has all the properties of the PDF (Pope, 1985). The transport equation for the VFDF is obtained by applying the filter to the equation governing the evolution of fine-grained density (Gicquel, 2001). The effects of SGS convection in physical space appear in a closed form in this equation. However, the convective effects in the velocity space due to SGS pressure gradient and SGS diffusion need to be modeled. For closure of these terms, the generalized Langevin model (GLM) (Haworth and Pope, 1986; Pope, 1994) is employed,

$$\begin{aligned}\frac{DP_L}{Dt} = &-\frac{\partial}{\partial x_k}[(v_k - \langle u_k\rangle_L)P_L] + \frac{\partial\langle p\rangle_L}{\partial x_i}\frac{\partial P_L}{\partial v_i} - \frac{\partial\langle\sigma_{ik}\rangle_L}{\partial x_k}\frac{\partial P_L}{\partial v_i} \\ &- \frac{\partial}{\partial v_i}[\, G_{ij}\,(v_j - \langle u_j\rangle_L)\,P_L\,] + \frac{1}{2}\,C_0\,\varepsilon\,\frac{\partial^2 P_L}{\partial v_i \partial v_i},\end{aligned} \tag{4}$$

where $\frac{D}{Dt} = \frac{\partial}{\partial t} + \langle u_k\rangle_L \frac{\partial}{\partial x_k}$, and the two terms G_{ij} and ε jointly represent the SGS pressure-strain and SGS dissipation,

$$G_{ij} = -\,\omega\,\left(\frac{1}{2} + \frac{3}{4}C_0\right)\,\delta_{ij},\;\; \varepsilon = C_\varepsilon\, k^{3/2}/\Delta_L,\;\; \omega = \varepsilon/k. \tag{5}$$

In this model ω is the SGS mixing frequency, $k = \frac{1}{2}\tau_L(u_i, u_i)$ is the SGS kinetic energy, and ε is the SGS dissipation rate. In Reynolds averaged simulations, typically $C_\varepsilon \approx 1$, and $C_0 \approx 2.1$.

In addition to VFDF, three other LES are conducted with (1) no SGS model, (2) the Smagorinsky SGS closure (Smagorinsky, 1963), and (3) the dynamic Smagorinsky (Germano *et al.*, 1991; Germano, 1992; Lilly, 1992) model. The no model refers to the case in which the contribution of the SGS is completely ignored, *i.e.* $\tau_L(u_i, u_j) = 0$.

3. Numerical Solution Procedure

The solution of the VFDF transport equation provides all the statistical information pertaining to the velocity vector. The most convenient means of solving this equation is via the Lagrangian Monte Carlo scheme (Pope, 1985; Pope, 1994). To do so, the general diffusion process is considered via the following system of stochastic differential equations (SDEs) (Pope, 1985; Haworth and Pope, 1986),

$$\begin{aligned} d\mathcal{U}_i(t) &= \left[\left(-\frac{\partial\langle p\rangle_L}{\partial x_i} + \frac{\partial\langle\sigma_{ik}\rangle_L}{\partial x_k}\right) + G_{ij}\,(\mathcal{U}_j(t) - \langle u_j\rangle_L)\right]\,dt + \sqrt{C_0\varepsilon}\,dW_i^v(t) \\ d\mathcal{X}_i(t) &= \mathcal{U}_i(t)\,dt, \end{aligned} \tag{6}$$

where $\mathcal{X}_i$ and $\mathcal{U}_i$ are probabilistic representations of the position and the velocity, respectively; and W_i^v denotes independent Wiener-Lévy processes (Karlin and Taylor, 1981). The corresponding Fokker-Planck equation for this diffusion process is the same as the VFDF transport equation. With the Lagrangian description, the VFDF is represented by an ensemble of Monte Carlo particles. Each of these particles carries information pertaining to its velocity and position. This information is updated via temporal integration of Eq. (6). The statistics are evaluated by consideration of the ensemble of particles in a "finite volume" centered at a spatial location. This finite volume is characterized by a cubic box of length Δ_E containing N_E Monte Carlo particles.

The "mean field solver" is based on the "compact parameter" finite difference scheme (Carpenter, 1990) with a fourth order spatial accuracy and a second order symmetric predictor-corrector sequence for time discretization. All the finite difference operations are conducted on fixed and equally sized grid points with spacings Δ. The transfer of information from these points to the location of the Lagrangian particles is conducted via interpolation. The mean-field solver also determines the filtered velocity field. That is, there is a "redundancy" in the determination of the first filtered moments as both the finite difference and the Monte Carlo procedures provides the solution of this field. This redundancy is actually very useful in monitoring the accuracy of the simulated results (Jaberi *et al.*, 1999; Muradoglu *et al.*, 1999). The DNS and all the other LES (via the no-model, Smagorinsky, and the dynamics Smagorinsky) are conducted with the same finite-difference scheme.

4. Results

Simulations are conducted of a three-dimensional (3D) temporally developing mixing layer. This layer consists of two parallel streams traveling in opposite directions with the same speed (Moser and Rogers, 1992). A hyperbolic tangent profile is utilized to assign the velocity distribution at the initial time. The coordinates x, y, z denote the streamwise, cross-stream, and spanwise directions, respectively. The flowfield is initialized with a procedure somewhat similar to that considered previously (Vreman *et al.*, 1997) which results in the formation of two successive vortex pairings and strong three-dimensionality. Simulations are conducted on 193^3 and 33^3 points for DNS and LES, respectively. For filter, a top-hat function of width $\Delta_L = 2\Delta$ is used. No attempt is made to investigate the sensitivity of the results to the filter function (Vreman *et al.*, 1994) or the size of the filter. Simulations are conducted with $C_\varepsilon = 1$, $C_0 = 2.1$, $\Delta_E = \Delta/2$, $N_E = 40$, and with a uniform "weight" (Pope, 1985) of the Monte Carlo particles.

Figures 1 and 2 show the contours of the spanwise and the streamwise components of the vorticity field, respectively. By this time, the flow has gone through several pairings and exhibits strong 3D effects. This is evident by the formation of large scale spanwise rollers with presence of counter-rotating streamwise vortex pairs in all the simulations. The results via the no-model indicate too many small-scale structures which clearly are not captured accurately on the coarse grid. The amount of SGS diffusion with the Smagorinsky model is very significant at initial times. Due to this dissipative characteristics of the model, the predicted results are too smooth and only contain the large scale structures. The vortical structures as depicted by the dynamic Smagorinsky and the VFDF are very similar and predict the DNS results better than the other two models. But both models yield less fine structures as compared to DNS. The Reynolds averaged values of the simulated data (not shown) also indicate the dissipative nature of the Smagorinsky model resulting in a slow growth of the layer. As a result, this model does not predict the spread and the peak value of the resolved Reynolds stresses. The VFDF predicts both the spread and the peak values reasonably well, except for small C_ε values. In this case, the amount of energy in the resolved scale decreases too much in favor of the increase of the SGS stress.

5. Acknowledgments

This work is sponsored by the U.S. Air Force Office of Scientific Research under Grant F49620-00-1-0035 to SUNY-Buffalo and Grant F49620-00-1-0171 to Cornell University. Dr. Julian M. Tishkoff is the Program Manager for both these grants. Additional support for the work at SUNY-Buffalo is provided by the NASA Langley Research Center under Grant NAG-1-2238 with Dr. J. Philip Drummond as the Technical Monitor. Acknowledgment is also made to the Donors of the Petroleum Research Funds administrated by the American Chemical Society for their support under Grant ACS-PRF 36981-AC9. Computational resources are provided by the NCSA at the University of Illinois at Urbana and by the CCR at SUNY-Buffalo.

References

Carpenter, M. H. (1990). A high-order compact numerical algorithm for supersonic flows. In Mortron, K. W., editor, *Proc. 12th International Conference on Numerical Methods in Fluid Dynamics*, volume 371 of *Lecture Notes in Physics*, pages 254–258. Springer-Verlag.

Colucci, P. J., Jaberi, F. A., Givi, P., and Pope, S. B. (1998). Filtered density function for large eddy simulation of turbulent reacting flows. *Phys. Fluids* **10**, 499–515.

Gao, F. and O'Brien, E. E. (1993). A large-eddy simulation scheme for turbulent reacting flows. *Phys. Fluids A* **5**, 1282–1284.

Garrick, S. C., Jaberi, F. A., and Givi, P. (1999). Large eddy simulation of scalar trans-

port in a turbulent jet flow. In Knight, D. and Sakell, L., editors, *Recent Advances in DNS and LES*, volume 54 of *Fluid Mechanics and its Applications*, pages 155–166. Kluwer Academic Publishers, The Netherlands.

Germano, M., Piomelli, U., Moin, P., and Cabot, W. H. (1991). A dynamic subgrid-scale eddy viscosity model. *Phys. Fluids* **A3**, 1760–1765.

Germano, M. (1992). Turbulence: The filtering approach. *J. Fluid Mech.* **238**, 325–336.

Gicquel, L. Y. M. (2001), *Velocity Filtered Density Function for Large Eddy Simulation of Turbulent Flows*. Ph.D. Dissertation, Department of Mechanical and Aerospace Engineering, State University of New York at Buffalo, Buffalo, NY.

Geurts, B. J., editor. (2001). *Modern Simulation Strategies for Turbulent Flow*. R. T. Edwards, Inc., Philadelphia, PA.

Haworth, D. C. and Pope, S. B. (1986). A generalized Langevin model for turbulent flows. *Phys. Fluids* **29**, 387–405.

Jaberi, F. A., Colucci, P. J., James, S., Givi, P., and Pope, S. B. (1999). Filtered mass density function for large eddy simulation of turbulent reacting flows. *J. Fluid Mech.* **401**, 85–121.

James, S. and Jaberi, F. A. (2000). Large scale simulations of two-dimensional non-premixed methane jet flames. *Combust. Flame* **123**, 465–487.

Karlin, S. and Taylor, H. M. (1981). *A Second Course in Stochastic Processes*. Academic Press, New York, NY.

Lilly, D. K. (1992). A proposed modification of the Germano sub-grid closure method. *Phys. Fluids* **A 4**, 633–635.

Moser, R. D. and Rogers, M. M. (1992). The three-dimensional evolution of a plane mixing layer: the Kelvin-Helmholtz rollup. *J. Fluid Mech.* **243**, 183–226.

Muradoglu, M., Jenny, P., Pope, S. B., and Caughey, D. A. (1999). A consistent hybrid-volume/particle method for the PDF equations of turbulent reactive flows. *J. Comp. Phys.* **154**, 342–371.

O'Brien, E. E. (1980). The probability density function (PDF) approach to reacting turbulent flows. In Libby, P. A. and Williams, F. A., editors, *Turbulent Reacting Flows*, chapter 5, pages 185–218. Springer-Verlag, Heidelberg.

Poinsot, T. and Veynante, D. (2001). *Theoretical and Numerical Combustion*. R. T. Edwards, Inc., Philadelphia, PA.

Pope, S. B. (1985). PDF methods for turbulent reacting flows. *Prog. Energy Combust. Sci.* **11**, 119–192.

Pope, S. B. (1990). Computations of turbulent combustion: Progress and challenges. In *Proceedings of 23rd Symp. (Int.) on Combustion*, pages 591–612. The Combustion Institute, Pittsburgh, PA.

Pope, S. B. (1994). Lagrangian PDF methods for turbulent flows. *Ann. Rev. Fluid Mech.* **26**, 23–63.

Pope, S. B. (2000). *Turbulent Flows*. Cambridge University Press, Cambridge, UK.

Réveillon, J. and Vervisch, L. (1998). Subgrid scale turbulent micromixing: dynamic approach. *AIAA J.* **36**, 336–341.

Sagaut, P. (2001). *Large Eddy Simulation for Incompressible Flows*. Springer, New York.

Smagorinsky, J. (1963). General circulation experiments with the primitive equations. I. The basic experiment. *Monthly Weather Review* **91**, 99–164.

Tong, C. (2001). Measurements of conserved scalar filtered density function in a turbulent jet. *Phys. Fluids* **13**, 2923–2937.

Vreman, B., Geurts, B., and Kuerten, H. (1994). Realizability conditions for the turbulent stress tensor in large-eddy simulation. *J. Fluid Mech.* **278**, 351–362.

Vreman, B., Geurts, B., and Kuerten, H. (1997). Large-eddy simulation of the turbulent mixing layer. *J. Fluid Mech.* **339**, 357–390.

Zhou, X. Y. and Pereira, J. C. F. (2000). Large eddy simulation (2D) of a reacting plan mixing layer using filtered density function. *Flow, Turbulence and Combustion* **64**, 279–300.

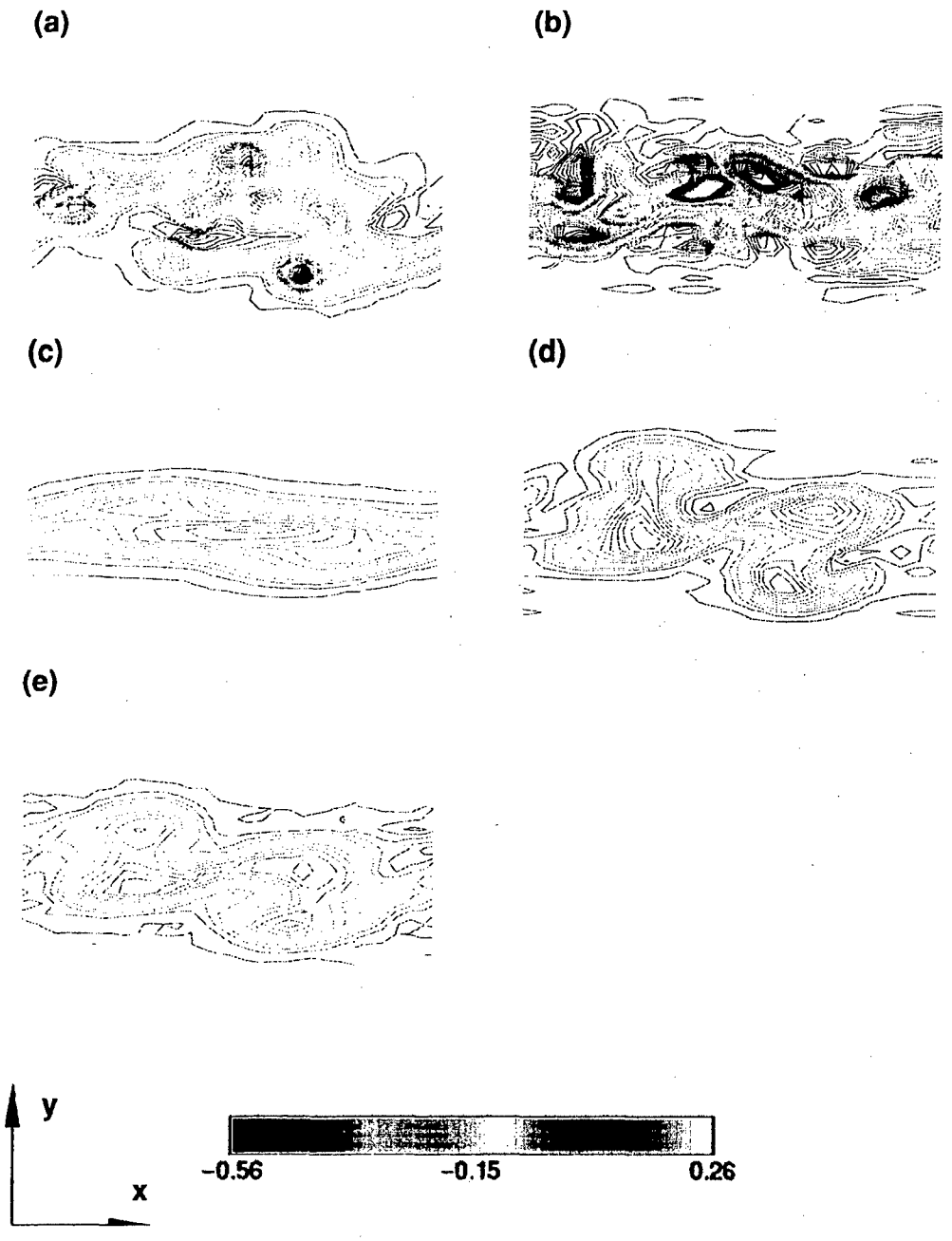

Figure 1. Contour plots of the spanwise component of the vorticity. (a) Filtered DNS, (b) no model, (c), Smagorinsky model, (d) dynamic Smagorinsky model, (e) VFDF.

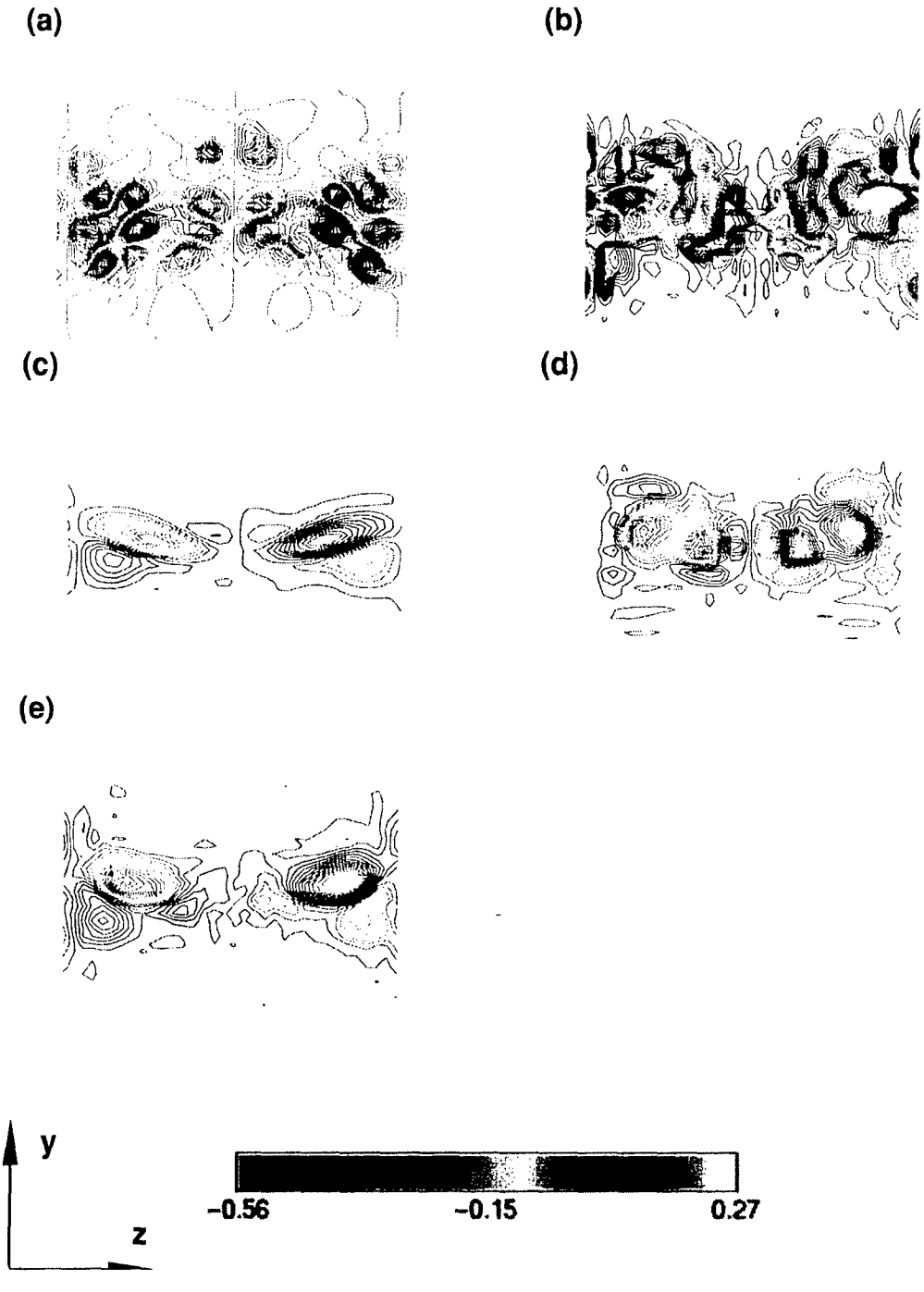

Figure 2. Contour plots of the streamwise component of the vorticity vector. (a) Filtered DNS, (b) no model, (c) Smagorinsky model, (d) dynamic Smagorinsky model, (e) VFDF.